University of Tehran Press

Journal of the Earth and Space Physics

Homepage: https://jesphys.ut.ac.ir

Vol. 49, No. 4, Winter 2024, P. 27-35

(Research Article)

Improving the Accuracy of Analytical Downward Continuation of Terrestrial Gravity Anomalies

Goli, M.[1]

1. Department of Geotechnical and Transport Engineering, Faculty of Civil Engineering, Shahrood University of Technology, Shahrood, Iran.

Corresponding Author E-mail: goli@shahroodut.ac.ir

(Received: 1 May 2023, Revised: 3 June 2023, Accepted: 26 Sep 2023, Published online: 20 Feb 2024)

Abstract

The determination of the geoid using the Stokes integral involves transforming gravity data from their measurement altitude to the geoid/ellipsoid surface. This study focuses on improving the accuracy of analytical downward continuation (ADC) for reducing terrestrial gravity anomalies to the geoid. The ADC method uses the Taylor series and successive vertical gradients of the gravity anomalies. The Moritz integral formula, which is based on Poisson's integral, is used to derive the vertical gravity gradient. To enhance its accuracy, a mean vertical gradient is proposed by introducing an analytical formula based on planar approximation. This formula improves accuracy by 50%. Numerical analysis, using simulated free air anomalies up to harmonic degree/order 5540/5540, reveals that the difference between mean and point ADC results in geoidal height can be several decimeters. The study also finds that the ADC of 2'×2' anomalies remains stable even with different levels of noise, while the Taylor series of 1'×1' gravity anomalies diverges.

Keywords: Analytical Downward Continuation, Mean Vertical Gradient, Gravity Anomaly, Taylor Series.

1. Introduction

The use of Stokes's formula for determining the geoid requires that the gravity anomalies, which are boundary values, be referred to the geoid. Therefore, gravity reduction is necessary to harmonically downward continuation (DC) of the gravity anomalies from the Earth's surface to the geoid. DC is a challenging stage in solving geodetic boundary value problems, as it is inherently ill-posed. However, for discrete data, instability is dependent on the presence of high-frequency components in data, including measurement noise.

Different techniques are utilized to perform DC such as: least squares collocation (LSC), the Poisson integral and analytical downward continuation (ADC) methods. LSC can reduce gravity anomalies between two arbitrary surfaces using the construction of the 3D covariance function (Forsberg, 1987; Zhao et al., 2018; Li et al., 2022). Poisson integral, which numerically solves a Fredholm's integral equation of the first-kind, has been examined by Heiskanen and Moritz (1967), Vaníček et al. (1996), Martinec (1996), Sun and Vaníček (1998), Goli et al. (2011), Sebera et al. (2014), Vaníček et al. (2017), Foroughi et al (2018), Sajjadi et al. (2021), and Li et al. (2022). Employing Taylor series expansion, the ADC has been described by Moritz (1980), Sideris (1987), Huang et al. (2003), and Li et al. (2022).

The LSC and Poisson integral methods have a major weakness that requires solving a large system of linear equations, which can be computationally challenging for dense gravity data. Additionally, the DC of dense gravity data using Poisson integral yields an ill-posed problem that should be regularized in appropriate way. Several studies have investigated the instability of DC of terrestrial gravity data using Poisson approach. Martinec (1996) demonstrated that the DC of gravity anomalies with spacing less than 1 km is unstable. Goli et al. (2018) used the analysis of the Picard condition to demonstrate that the DC of Helmert anomalies with spacing less than 2 km in mountainous regions is unstable. Sajjadi et al. (2021) analyzed gravity data in Ireland and showed that the DC of data with spacing less than 500 m is unstable.

The ADC has been widely used in geophysical studies for gravity reduction between two surfaces, assuming a planar approximation of topography (Xu et al., 2007; Zeng et al., 2013; Zeng et al., 2015; Zhang et al., 2016, 2018). Moritz (1980) used the Taylor series to solve the Molodensky

Cite this article: Goli, M. (2024). Improving the Accuracy of Analytical Downward Continuation of Terrestrial Gravity Anomalies. *Journal of the Earth and Space Physics*, 49(4), 27-35. DOI: http//doi.org/10.22059/jesphys.2023.358262.1007520

Publisher: University of Tehran Press.
DOI: http//doi.org/10.22059/jesphys.2023.358262.1007520

Print ISSN: 2538-371X
Online ISSN: 2538-3906

boundary value problem for reduction of gravity anomaly from the telluroid to the point level for the determination of the height anomaly, which is called analytical downward continuation by him.

ADC involves using successive vertical gradients of gravity. However, calculating these gradients as a derivative operator amplifies high-frequency components of data. Instability in the gravity anomaly ADC problem can cause the Taylor series to diverge. Various studies have investigated the instabilities of the Taylor series for ADC of gravity anomalies in geophysical studies. For example, see Zhang et al. (2013), Zeng et al. (2015), and Zhang et al. (2018). However, most of these studies are limited to the reduction of the gravity anomaly between two planar surfaces and are not practically useful for the terrestrial gravity data observed on the irregular surface of the Earth.

The numerical evaluation of the successive vertical gravity gradients is the heart of ADC and can be calculated from the data using various methods, such as numeric integration (Moritz, 1980; Huang et al., 2003; Li et al., 2022), computing from horizontal gradients (Fedi and Florio, 2002; Zhang et al., 2016), and Fast Fourier Transform (FFT) (Cooper, 2004; Xu et al., 2007; Pasteka et al., 2018). In geodetic applications, numeric integration is often preferred as it can be formulated for a spherical or ellipsoidal Earth.

The aim of this study is to improve the efficiency of the ADC method for continuing terrestrial gravity data. To achieve this goal, we introduce the mean vertical gradient operator and derive an analytical formula. In addition, we examine the kernel behavior and truncation error of the mean vertical gradient. Finally, we investigate the relationship between data spacing and the convergence of the Taylor series.

2. Theory

In a harmonic space, the gravity anomaly on the Earth's surface is obtained from the Taylor series expansion of the gravity anomaly on the geoid:

$$\Delta g(r_i,\Omega) = \Delta g(R,\Omega) + \frac{\partial \Delta g}{\partial h}\Big|_{r=R} h + \frac{1}{2}\frac{\partial^2 \Delta g}{\partial h^2}\Big|_{r=R} + \cdots, \quad (1)$$

where $\Omega = (\theta, \lambda)$ represents the surface coordinates of the point, R is the mean radius of the Earth, λ and θ are the longitude and latitude respectively. Using the approximation $\frac{\partial}{\partial h} \approx \frac{\partial}{\partial r}$, the vertical gradient of function f on the sphere can be obtained as (Heiskanen and Moritz ,1967):

$$\frac{\partial f(R,\Omega)}{\partial h} = -\frac{2}{R} f(R,\Omega) + \frac{R^2}{2\pi}\iint_\sigma \frac{f(R,\Omega') - f(R,\Omega)}{l_0^3} \mathrm{d}\sigma', \quad (2)$$

Where $l_0 = 2\,R \sin\frac{\psi}{2}$ is the spatial distance between two points on the geoid, and ψ is the spherical distance. In Equation (1), the gravity anomaly on the geoid $\Delta g(R,\Omega)$ cannot be directly calculated from the anomaly on the Earth's surface $\Delta g(r_i,\Omega)$. Moritz (1980) proposed an iterative method for calculating $\Delta g(R,\Omega)$ from Equation (1) as follows:

$$\Delta g(R,\Omega) = \sum_{n=0}^{\infty} g_i\,, \quad (3)$$

Where

$$g_0 = \Delta g(r,\Omega), \qquad g_n = -\sum_{m=1}^{n} h^m L_m(g_{n-m}),\ n > 1. \quad (4)$$

The function $L(\Delta g)$ is the vertical gradient operator defined in Equation (2). This operator has the following property [ibid]:

$$L_m = \frac{1}{n} L\,(L_{m-1})\,,\ n,m > 1\,. \quad (5)$$

Evaluating the series (3), even for the first few terms, requires the use of multiple gradient operators, resulting in significant increase in computational time. However, by performing some mathematical calculations, a simple formula for g_n can be derived:

$$g_0 = \Delta g(r,\Omega),\ g_n = -\frac{h}{n} L(g_{n-1}), n \geq 1. \quad (6)$$

In this equation, only one integration is utilized at each iteration. If all derivatives are obtained based on the term g_0, then the ADC takes the following form (Bjerhammar, 1969; long and Kaufman, 2013):

$$\Delta g(R,\Omega) = g_0 - hL[g_0] + \frac{h^2}{2!}L\big[L[g_0]\big] - \frac{h^3}{3!}L\Big[L\big[L[g_0]\big]\Big] + \cdots = g_0 + g_1 + g_2 + \cdots \quad (7)$$

3. Mean vertical gradient

If the gravity anomaly is provided on a regularly spaced grid, a straightforward approach for numerical integration of Equation (2) is to utilize the trapezoidal rule:

$$\frac{\partial f(R,\Omega_i)}{\partial h} = -\frac{2}{R} f(R,\Omega_i) + \sum_{i=1}^{N}\left[f(R,\Omega_j) - f(R,\Omega_i)\right] K(\psi)\ cos\,\varphi_j\,\Delta\varphi\,\Delta\lambda, \quad (8)$$

where $K(\psi) = \frac{R^2}{2\pi} l_0^{-3}(\Omega_i,\Omega_j)$, Here, $\Delta\varphi$ and $\Delta\lambda$ represent the grid steps in the longitudinal and latitudinal directions, respectively. In this study, we refer to the kernel $K(\psi)$ as the point kernel as it is calculated at the center of geoid cell. However, due to a large variation of $K(\psi)$ when $\psi \to 0$, Equation (8) has a large discretization error for small spherical distances. Hirt et al. (2011) demonstrated that using the concept of mean kernels for convolution integrals can significantly reduce discretization error. Goli et al. (2011) showed that the mean kernel of the Poisson integral offers much higher accuracy than its point kernel counterpart.

We define the mean vertical gradient operator of mean anomaly as:

$$\frac{\partial \overline{\Delta g}(R,\Omega)}{\partial h} = -\frac{2}{R}\overline{\Delta g}(R,\Omega) + \frac{R^2}{2\pi}\iint_{\sigma} \overline{\Delta g}(R,\Omega')\overline{K}(\psi)\mathrm{d}\sigma'. \quad (9)$$

$\overline{K}(\psi)$ is the mean kernel in each cell:

$$\overline{K}(\psi) = \frac{1}{8R^3}\int_{C_j} \sin^{-3}\frac{\psi}{2}\,\mathrm{d}\sigma'. \quad (10)$$

The average anomaly in each cell is represented by $\overline{\Delta g}$. The mean kernel $\overline{K}$ can be computed by numerically integrating over each cell C_j, but this approach is both time-consuming and singular at $\psi = 0$. Thus, to ensure accurate calculations and remove the singularity, we utilize its analytical solution in the local Cartesian system. The local Cartesian coordinate system can be defined as:

$$x = R\,(\varphi - \varphi_0),\ y = R\,(\lambda - \lambda_0)\cos\varphi. \quad (11)$$

The expression for the mean kernel in the Cartesian coordinate system can be written as:

$$\overline{K}(x,y,x',y') = \frac{1}{R^2}\int_{x_1}^{x_2}\int_{y_1}^{y_2} \frac{\mathrm{d}x'\mathrm{d}y'}{d^3(x,y,x',y')}, \quad (12)$$

where $d = \sqrt{(x-x')^2 + (y-y')^2}$ represents the distance between the computation point and the integration point on the geoid. By introducing the computation point as the origin of the coordinate system, the solution to the integral (12) can be derived as:

$$\overline{K}(x,y,x',y') = -\left|\left|\frac{d}{x'y'}\right|_{-R\Delta\varphi}^{+R\Delta\varphi}\right|_{-R\Delta\lambda\cos\varphi'}^{+R\Delta\lambda\cos\varphi'}. \quad (13)$$

The kernel $\overline{K}$ is not singular at $\psi = 0$. The planar approximation does not introduce a significant error since $\overline{K}$ attenuates at small distances.

Theoretically, integrals (2) and (8) cover the entire surface of the Earth. Practically, due to limited data coverage, these integrals are truncated at short distances. The truncation error can be calculated by using long-wavelength components of the gravity anomaly computed from a geopotential model. The truncation error for integral (8) is read:

$$FZ = \frac{R^2}{2\pi}\iint_{\psi>\psi_0} \overline{\Delta g}(R,\Omega')\overline{K}(\psi)\mathrm{d}\sigma' \approx \frac{R^2}{2\pi}\iint_{\psi>\psi_0} \Delta g(R,\Omega')K(\psi)\mathrm{d}\sigma', \quad (14)$$

where ψ_0 represents the integration radius. The Molodensky truncation coefficients (Molodenskij et al., 1962) can be utilized to compute the truncation error. By introducing the kernel $K^*(\psi)$, we obtain:

$$K^*(\psi) = \begin{cases} 0, & \psi \le \psi_0 \\ K(\psi), & \psi > \psi_0, \end{cases} \quad (15)$$

The truncation error is given by:

$$FZ = \frac{R^2}{2\pi}\int_{\alpha=0}^{2\pi}\int_{\psi=0}^{\pi} \Delta g(R,\Omega')K^*(\psi)\sin\psi\ \mathrm{d}\alpha\,\mathrm{d}\psi. \quad (16)$$

The spectral form of the kernel $K^*(\psi)$ is given by:

$$K^*(\psi) = \sum_{n=0}^{\infty}\frac{2n+1}{2}\,t_n\,P_n(\cos\psi). \quad (17)$$

The coefficients t_n are computed as:

$$t_n = \int_{\psi=0}^{\pi} K^*(\psi)\,P_n(\cos\psi)\sin\psi\,\mathrm{d}\psi = \int_{\psi=\psi_0}^{\pi} K^*(\psi)\,P_n(\cos\psi)\sin\psi\,\mathrm{d}\psi. \quad (18)$$

The integral (19) can be evaluated numerically. By substituting Equation (18) into integral (17), we obtain:

$$FZ = \frac{R^2}{2\pi}\int_{\alpha=0}^{2\pi}\mathrm{d}\alpha\int_{\psi=0}^{\pi}\Delta g(R,\Omega')\sum_{n=0}^{\infty}\frac{2n+1}{2}\,t_n\,P_n(\cos\psi)\sin\psi\,\mathrm{d}\psi. \quad (19)$$

The truncation error of the integral is given by:

$$FZ = GMR\sum_{n=0}^{\infty} t_n\,\Delta g_n, \quad (20)$$

where Δg_n is the n-th degree harmonic of the gravity anomaly is derived using an EGM. GM is the product of the gravitational constant and the mass of the Earth. Since the truncation error of the integral is due to the long-wavelength components of the kernel K, expansion (20) is only calculated up to low degrees such as $N = 360$.

4. Fast computation of mean kernel

The analytical formula (13) speeds up mean kernel computation, but ADC calculations are still time-consuming. To improve efficiency, FFT can be utilized. However, in this study, we employ the isotropic property of the kernel $\overline{K}$. The kernel $\overline{K}$ depends solely on the spherical distance ψ, and its value remains constant in each parallel for varying λ values. Hence, $\overline{K}$ only needs to be computed once per parallel, significantly reducing computation time. Huang et al. (2000) have already utilized this method for the fast evaluation of the Stokes integral.

ADC has a significant advantage in that it can perform downward continuation without the need to solve a system of linear equations. However, the series (7) can often diverge when data spacing decreases. To overcome the issue, one approach is to use a few initial terms to approximate the solution (Zhang et al., 2013) Truncated Taylor series are equivalent to applied regularization methods in Poisson's integral method.

5. Numerical results

To investigate the accuracy of ADC, knowledge of gravity anomalies on Earth and the geoid surface is required. The XGM2019e geopotential model (Zingerle et al., 2020) was used to generate the free air anomaly corresponding to harmonic degree/order 5540 in the test area, limited to 25°<φ<40° and 45°<λ<60°. The point heights were obtained from the SRTM mean DEM. Figure 1 displays the gravity anomaly on the Earth's surface.

First, we calculated the truncation coefficients for three integration radii: ψ_0=0.5°, 1°, and 1.5°. Then, we computed the truncation error of g_1 using the EGM2008 model (Pavlis et al., 2012) up to degree/order 360. It should be noted that the truncation error of second and higher terms is neglected due to their small values. Figure 2 illustrates the truncation error of g_1 for three integration radii: ψ_0 =0.5°, 1° and 1.5°. According to this figure, for an integration radius of 1.5°, the average error caused by the far-zone effect is less than 0.1 mGal. Furthermore, our computations indicate that degree $N = 360$ is sufficient to compute the far zone contribution.

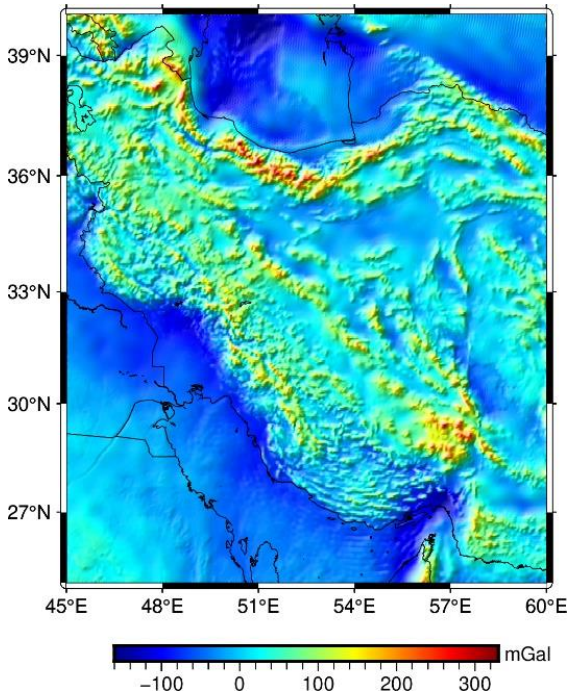

Figure 1. The surface free-air anomaly computed from the XGM2019e model up to degree/order 5540.

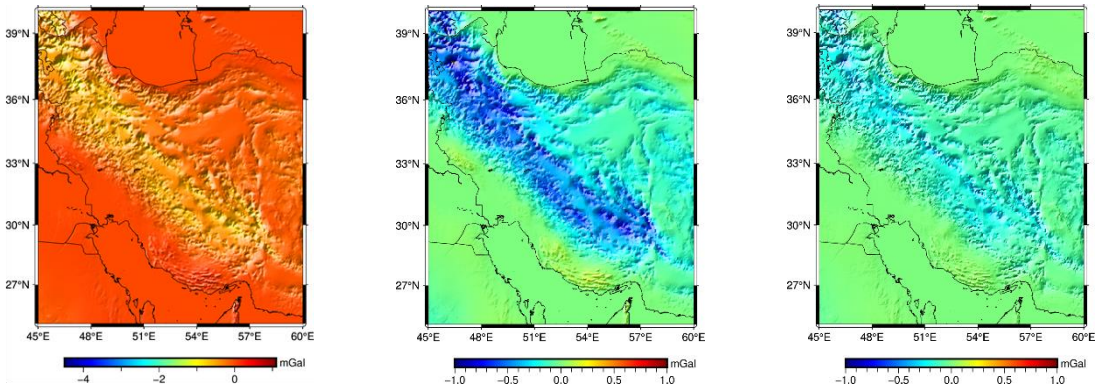

min=-4.5, max=0.8, mean=-0.4, STD=0.5 min=-1.1, max=0.2, mean=-0.1, STD=0.1 min=-0.5, max=0.1, mean=-0.0 STD=0.09

Figure 2. The truncation error of g_1 for integration radii of $\psi_0 = 0.5^\circ$ (left panel), $\psi_0 = 1^\circ$ (middle panel), and $\psi_0 = 1.5^\circ$ (right panel). Units: mGal.

To investigate the impact of the mean gradient operator, ADC performed using both point and mean kernels. ADC errors were computed by comparing the results with geoid anomalies from the XGM2019e model. Figures 2 and 3 display the ADC error for the point and mean kernels, respectively. The RMSE of the two kernels is approximately 9 and 14 mGal, indicating that the mean kernel reduces the ADC error by about 50%. The difference between the two kernels is significant in mountainous areas (Figure 4), with a standard deviation of the difference exceeding 5 mGal, equivalent to about 4 cm in geoid height, see Figure 5.

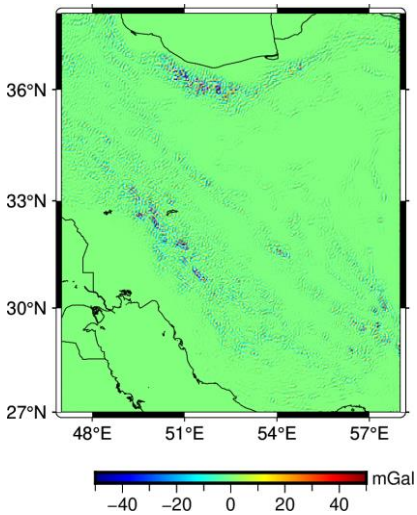

Figure 2. ADC error using the mean kernel. min=-170.9, max=713.8, mean=-0.4, STD=9.4 (mGal).

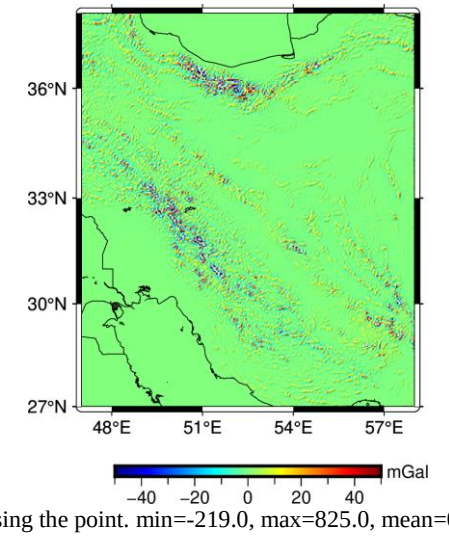

Figure 3. ADC error using the point. min=-219.0, max=825.0, mean=0.35, STD=14.3 (mGal).

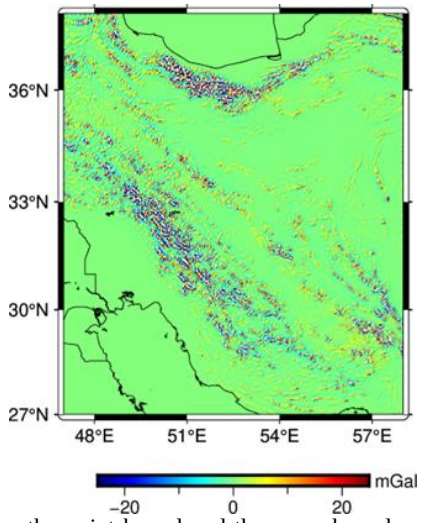

Figure 4. The difference in ADC using the point kernel and the mean kernel. min=-191.85, max= 71.52, mean=-0.76, STD= 5.74 (mGal).

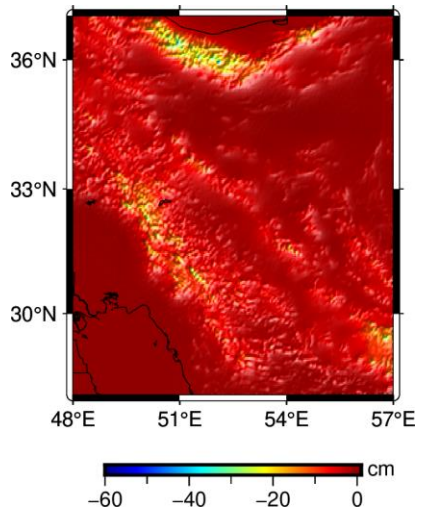

Figure 5. The difference in ADC between the point kernel and the mean kernel in the geoid height. min=-61.4, max=0.01, mean=-3.1, STD=3.9 (cm).

ADC of simulated 2'×2' gravity anomalies is a well-posed problem. For higher terms of the Taylor series, the error in ADC continuously decreases and the series converges after 10 terms with tolerance of 1μGal. However, the ADC of simulated 1'×1' gravity data diverges. It is important to note that the convergence of the Taylor series imply that the RMSE of results necessarily decrease for higher terms. For diverge series, after a few initial terms, the RMS decreases and then increases uniformly with higher terms. This phenomenon is comparable to semi-convergency that usually occurs in iterative solving of ill-posed problems (Goli et al., 2018). Figure 6 displays the RMSE of ADC for noise free 2'×2' and 1'×1' data for various numbers of Taylor series terms. According to the figure, semi-convergence occurs in the Taylor series of ADC for 1'×1' data. The RMS error decreases until the third term and then increases regularly due to the effect of high-frequency components in the data.

To investigate the impact of measurement noise on the ADC results and the convergence of the Taylor series, white noise with standard deviation 1.0, 2.0 and 5 mGal was added to the 2'×2' anomalies. Figure 7 shows the RMSE of ADC with mean kernel for different terms of the Taylor series, with and without noise. The figure demonstrates that even with a 5 mGal noise, the downward continuation remains convergent. The results shown in Figures 6 and 7 suggest that grid spacing is a more critical factor for the stability of the ADC compared to the noise in the data.

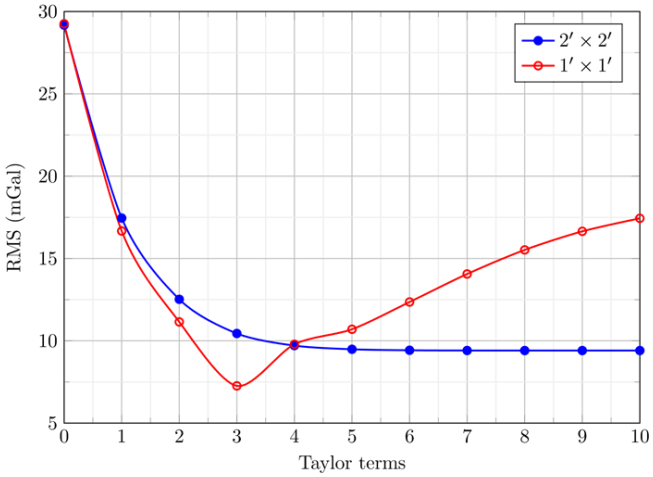

Figure 6. RMSE of ADC for noise free data.

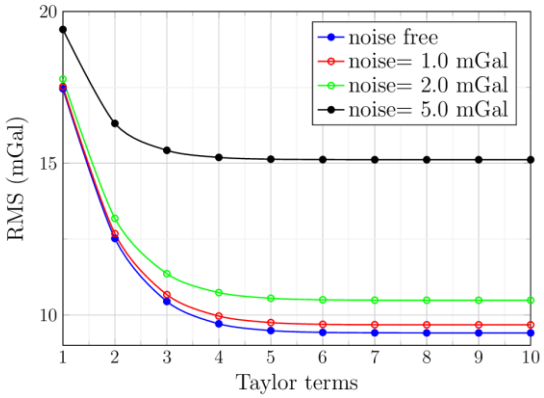

Figure 7. RMSE of ADC for noisy data.

6. Conclusion

The determination of the geoid by Stokes's integral requires the downward continuation of terrestrial gravity data from the Earth's surface onto the surface geoid or ellipsoid. However, this procedure is known to be unstable. In this study, the analytical downward continuation method was tested using simulated free-air anomalies.

The accuracy of ADC was improved by introducing the mean vertical gradient operator, and an analytical formula for its calculation was presented to speed up computations. Numerical experiments were performed using two regular grids with resolutions of 1'×1' and 2'×2', with different levels of noise. The results showed that the mean kernel improves the accuracy of ADC by up to 50% compared to the point kernel. The far-zone contribution of ADC did not exceed 0.1 mGal for a radius of 1.5°. The ADC of both free and noisy 2'×2' grids was found to be stable. However, the Taylor series of ADC for the 1'×1' grid is diverged, and the results show that the instability of ADC depends more on the grid spacing than the noise level.

References

Bjerhammar, A. (1969). On the boundary value problem of physical geodesy. *Tellus*, 21(4), 451-516, doi: 10.1111/j.2153-3490.1969.tb00460.x.

Cooper, G. (2004). The stable downward continuation of potential field data. *Exploration Geophysics*, 35(3), 260-265. doi: 10.1071/EG04260.

Fedi, M., & Florio, G. (2002). A stable downward continuation by using the ISVD method. *Geophysical Journal International*, 151(1), 146-156. doi: 10.1190/1.1450821.

Foroughi, I., Vaníček, P., Kingdon, R.W., Goli, M., Sheng, M., Afrashte, Y., Novak, P., & Santos, C.M. (2018). Sub-centimetre geoid. *Journal of Geodesy*, 92(2), 111-123. doi: 10.1007/s00190-017-1075-5.

Forsberg, R. (1987). A new covariance model for inertial gravimetry and gradiometry. *Journal of Geophysical Research: Solid Earth*, 92(B2), 1305–

1310.

Goli, M., Foroughi, I., & Novak, P. (2018). On estimation of stopping criteria for iterative solutions of gravity downward continuation. *Canadian Journal of Earth Sciences*, 55(4), 397-405. doi: 10.1139/cjes-2017-0208.

Goli, M., Najafi-Alamdari, M., & Vaníček, P. (2011). Numerical behaviour of the downward continuation of gravity anomalies. *Studia Geophysica et Geodaetica*, 55(2), 191-202. doi: 10.1007/s11200-011-0011-8.

Li, X., Huang J., Klees, R., Forsberg, R., Willberg, M., Slobbe, D.C., Hwang, C., & Pail, R. (2022). Characterization and stabilization of the downward continuation problem for airborne gravity data. *Journal of Geodesy*, 96(18), doi: 10.1007/s00190-022-01607-y.

Hirt, C., Featherstone, W.E., & Claessens, S.J. (2011). On the accurate numerical evaluation of geodetic convolution integrals. *Journal of Geodesy*, 85(8), 519-538. doi: 10.1007/s00190-011-0451-5.

Heiskanen, W.A., & Moritz, H. (1967). Physical Geodesy. W.H. Freeman and Company, San Francisco, 364 p.

Huang, J., Sideris, M.G., Vaníček, P., & Tziavos, I.N. (2003). Numerical investigation of downward continuation techniques for gravity anomalies. *Bollettino di Geodesia e Scienze Affini*, 62(1), 33-48.

Huang, J., Vaníček, P., & Novák, P. (2000). An alternative algorithm to FFT for the numerical evaluation of Stokes's integral. *Studia Geophysica et Geodaetica*, 44(4), 374-380. doi: 10.1023/A:1022160504156.

Long, L.T., & Kaufmann, R.D. (2013). *Acquisition and analysis of terrestrial gravity data*. Cambridge University Press.

Martinec, Z. (1996). Stability investigations of a discrete downward continuation problem for geoid determination in the Canadian Rocky Mountains. *Journal of Geodesy*, 70(12), 805-828. doi: 10.1007/s001900050069.

Molodenskij, M.S., Eremeev, V.F., & M.I., Yurkina. (1962). Method for Study of the External Gravitation Field and Figure of the Earth. Translated from Russian, Israel Program for Scientific Translations, Jerusalem.

Moritz, H. (1980). Advanced physical geodesy. Herbert Wichmann Verlag.

Pašteka, R., Kušnírák, D., & Karcol, R. (2018). Matlab tool REGCONT2: effective source depth estimation by means of Tikhonov's regularized downwards continuation of potential fields. *Contributions to Geophysics and Geodesy*, 48(3), 205-222. doi: 10.2478/congeo-2018-0010.

Pavlis, N.K., Holmes, S.A., Kenyon, S.C., & Factor, J.K. (2012). The development and evaluation of the Earth Gravitational Model 2008 (EGM2008). *Journal of Geophysical Research: Solid Earth*, 117(B4). doi: 10.1029/2011JB008916.

Sajjadi, S., Martinec, Z., Prendergast, P., Hagedoorn, J., & Šachl, L. (2021). The stability criterion for downward continuation of surface gravity data with various spatial resolutions over Ireland. *Studia Geophysica et Geodaetica*, 65(1), 59-76. doi: 10.1007/s11200-020-0769-7.

Sebera, J., Šprlák, M., Novák, P., Bezděk, A., & Vaľko, M. (2014). Iterative Spherical Downward Continuation Applied to Magnetic and Gravitational Data from Satellite. *Surveys in Geophysics*, 35(4), 941-958. doi: 10.1007/s10712-014-9285-z.

Sideris, M.G. (1987). Spectral methods for the numerical solution of Molodensky's problem. University of Calgary, *Ph.D. thesis*.

Sun, W., & Vaníček, P. (1998). On some problems of the downward continuation of the 5' × 5' mean Helmert gravity disturbance. *Journal of Geodesy*, 72(7), 411-420. doi: 10.1007/s001900050216.

Vaníček, P., Sun, W., Ong, P., Martinec, Z., Najafi, M., Vajda, P., & ter Horst, B. (1996). Downward continuation of Helmert's gravity. *Journal of Geodesy*, 71(1), 21-34. https://doi.org/10.1007/s001900050072.

Vaníček, P., Novák, P., Sheng, M., Kingdon, R., Janák, J., Foroughi, I., Martinec, Z., & Santos, M. (2017). Does Poisson's downward continuation give physically meaningful results?. *Studia Geophysica et Geodaetica*, 61(3), 412-428. doi: 10.1007/s11200-016-1167-z.

Xu, S.-z., Yang, J., Yang, C., Xiao, P., Chen, S., & Guo, Z. (2007). The iteration method for downward continuation of a potential field from a horizontal plane.

Geophysical Prospecting, 55(6), 883-889. doi: 10.1111/j.1365-2478.2007.00634.x.

Zeng, X., Liu, D., Li, X., Chen, D., & Niu, C. (2015). An improved regularized downward continuation of potential field data. *Journal of Applied Geophysics*, 106, 114-118. Doi: 10.1016/j.jappgeo.2015.02.011.

Zeng, X., Li, X., Su, J., Liu, D., & Zou, H. (2013). An adaptive iterative method for downward continuation of potential-field data from a horizontal plane. *Geophysics*, 78(4), J43-J52. doi: 10.1190/1.3237432.

Zhang, C., Lü, Q., Yan, J., & Qi, G. (2018). Numerical solutions of the mean-value theorem: new methods for downward continuation of potential fields. *Geophysical Research Letters*, 45(8), 3461-3470. doi: 10.1002/2018GL076995.

Zhang, H., Ravat, D., & Hu, X. (2013). An improved and stable downward continuation of potential field data: The truncated Taylor series iterative downward continuation method. *Geophysics*, 78(2), J75-J86. 10.1190/geo2012-0145.1.

Zhang, Y., Wong, Y.S., & Lin, Y. (2016). BTTB–RRCG method for downward continuation of potential field data. *Journal of Applied Geophysics*, 126, 74-86, doi: 10.1016/j.jappgeo.2015.12.001.

Zhao, Q., Xu, X., Forsberg, R., & Strykowski, G. (2018). Improvement of Downward Continuation Values of Airborne Gravity Data in Taiwan. *Remote Sensing*, 10, 12.

Zingerle, P., Pail, R., Gruber, T., & Oikonomidou, X. (2020). The combined global gravity field model XGM2019e. *Journal of Geodesy*, 94(7), 66. doi: 10.1007/s00190-020-01398-0.